

Terahertz wave generation from liquid water films via laser-induced breakdown

Yiwen E, Qi Jin, Anton Tcypkin, and X.-C. Zhang

Citation: *Appl. Phys. Lett.* **113**, 181103 (2018); doi: 10.1063/1.5054599

View online: <https://doi.org/10.1063/1.5054599>

View Table of Contents: <http://aip.scitation.org/toc/apl/113/18>

Published by the [American Institute of Physics](#)

Articles you may be interested in

[Gain dynamics in a heterogeneous terahertz quantum cascade laser](#)

Applied Physics Letters **113**, 181102 (2018); 10.1063/1.5049384

[Observation of broadband terahertz wave generation from liquid water](#)

Applied Physics Letters **111**, 071103 (2017); 10.1063/1.4990824

[Charge and thermal modeling of a semiconductor-based optical refrigerator](#)

Applied Physics Letters **113**, 181105 (2018); 10.1063/1.5049376

[Terahertz wave emission from a liquid water film under the excitation of asymmetric optical fields](#)

Applied Physics Letters **113**, 261101 (2018); 10.1063/1.5064644

[Broadband visible-to-telecom wavelength germanium quantum dot photodetectors](#)

Applied Physics Letters **113**, 181101 (2018); 10.1063/1.5052252

[Terahertz-driven ultrafast recovery of plasmon resonance in photoexcited nanoantennas on GaAs](#)

Applied Physics Letters **113**, 171103 (2018); 10.1063/1.5048011



Measure Ready
M91 FastHall™ Controller

A revolutionary new instrument
for complete Hall analysis

Lake Shore
CRYOTRONICS

Terahertz wave generation from liquid water films via laser-induced breakdown

Yiwen E,¹ Qi Jin,¹ Anton Tcypkin,² and X.-C. Zhang^{1,2,3,a)}

¹The Institute of Optics, University of Rochester, Rochester, New York 14627, USA

²ITMO University, Saint-Petersburg 197101, Russia

³Beijing Advanced Innovation Center for Imaging Technology, Capital Normal University, Beijing 100037, China

(Received 31 August 2018; accepted 20 October 2018; published online 1 November 2018)

Understanding the physics of terahertz (THz) wave generation from water is essential for developing liquid THz sources. This letter reports detailed experimental measurements of THz wave emission by focusing intense laser pulses onto water films. The simulation based on a ponderomotive force-induced dipole is supported by the observation of the THz intensity dependence on the laser incidence angle. This work provides fundamental insights into the THz wave generation process in water and an alternative perspective for studying laser-induced breakdown in liquids. *Published by AIP Publishing.* <https://doi.org/10.1063/1.5054599>

Laser-induced breakdown in gases, liquids, or solids is widely used for the fundamental and applied research in the laser-matter interaction community.^{1–3} Accelerated charged particles in a laser-induced plasma act like broadband electromagnetic sources and cover the spectrum from microwaves to X-rays.^{4–7} Light emission from ionized materials not only provides the spectral signatures of a plasma but also characterizes its material properties. Air plasma has been experimentally demonstrated to radiate terahertz (THz) waves with fields greater than 8 MV/cm.⁸ Such intense field strength makes the measurement of THz field-induced dynamics feasible in ultrafast spectroscopy.⁹

Recently, broadband THz wave generation from a gravity-driven, free-flowing water film¹⁰ and from liquids in a cuvette¹¹ has been experimentally demonstrated through ionizing liquid media. Compared with ambient air, liquid water has much lower ionization energy (6.5 eV) but 3 orders higher molecular density,^{12–14} which means that more charged particles can be provided in the same ionized volume. Compared with solid crystals, phase matching conditions and crystal phonon absorption¹⁵ are avoided in the generation process, which significantly limit the bandwidth of the THz pulse generated from solid sources. Additionally, the breakdown in liquids is not a permanent damage, which will be naturally erased through electron-ion recombination. Liquid fluidity can also provide a fresh interaction area for the next pulse. All these superiorities make liquids a promising THz source. Therefore, it is imperative to investigate the mechanism of THz wave generation from water.

In this paper, the flipped THz waveforms are experimentally observed when the laser is incident on the water film at opposite incidence angles. This observation supports a ponderomotive force-induced dipole in the laser propagation direction. Accordingly, THz wave intensity as a function of the laser incidence angle and the detection angle is derived in both forward and backward directions, including interface

refractions and THz signal attenuation in a water film. Furthermore, the linear increase in THz intensity with laser pulse energy is discussed.

The experimental setup uses a Ti:sapphire amplified laser with 3 mJ pulse energy, horizontal polarization, 800 nm center wavelength, and 1 kHz repetition rate. It is focused into a 120- μ m water film by a 2-in. focal length lens ($f/4$) ionizing water molecules near the focus. The laser beam diameter is 10 mm. Both a 2-mm thick $\langle 110 \rangle$ oriented ZnTe crystal configured for electro-optical (EO) sampling¹⁶ and a commercially available Golay cell are used for the THz wave detection. An illustration of incidence angle α for the laser beam and detection angle β for the detector is shown in Fig. 1(a), where \hat{n} is the surface normal of the water film. These two angles are defined with respect to the laser propagation direction (z -axis) and can be changed through rotating the film and the detector, respectively. The sign of the angle is negative/positive if it is measured clockwise/counter-clockwise from the z -axis.

A liquid jet with a pressure of 30 psi is used to create a 5-mm wide, 120- μ m thick free-standing water film, as shown in Fig. 1(b). The thickness is measured by an auto-correlation system.¹⁷ Compared to a gravity-driven, wire-guided water film,¹⁰ the jet film can bear higher laser power without disrupting the water flow. The gravity driven, wire-guided film can be broken under intense optical excitation, in which the surface tension could not restore the film before next the laser pulse comes. The relatively high flow rate of a jet benefits a stable thin film, which is crucial for generating intense THz waves. Based on our observations, the optimal laser pulse duration for the strongest THz signal is determined by the thickness of the water film. For a 120- μ m thick film, the pulse duration is tuned to 0.3 ps for maximizing the THz signal.

Figure 1(c) plots the THz waveforms generated from the water film with two opposite incidence angles ($\alpha = \pm 65^\circ$) and detected in the laser propagation direction. The corresponding spectrum is shown in the inset. The electric field strength is about 160 V/cm. Both the central wavelength and

^{a)}Author to whom correspondence should be addressed: xicheng.zhang@rochester.edu

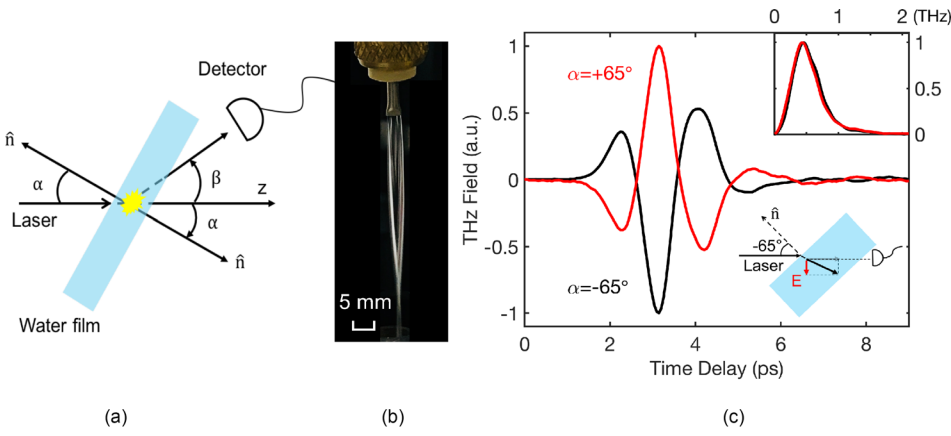


FIG. 1. (a) Illustration of incidence angle α and detection angle β . All angles are defined with respect to the z axis. (b) Photograph of a 120- μm thick water film formed by a water jet with a flat nozzle. The laser beam is focused into the center position of the film, which is relatively flat and stable. (c) THz waveforms generated from a water film with opposite incidence angles ($\alpha = \pm 65^\circ$). The corresponding spectra and dipole approximation illustration are shown in the insets.

the full width at the half maximum (FWHM) are about 0.5 THz. Therefore, the parameters at 0.5 THz are used in the following calculation.¹⁷ As shown in Fig. 1(c), the waveform keeps its amplitude but completely flips over when the incidence angle changes its sign. This observation applies to all the opposite incidence angles. It can be inferred that the dipole direction is along the propagation direction of the refracted laser beam, illustrated as a black arrow in Fig. 1(c). The detectable dipole projection reverses in the direction when the incidence angle changes its sign, which accounts for the flipped waveforms.

Figure 2(a) shows the cross-section diagram of the THz wave generation process in a water film. Laser pulses ionize water molecules at the focus through multiphoton absorption and cascade ionization after refracting at the air/water interface.¹⁸ In the ionized area, quasi-free electrons in water experience the ponderomotive force and move towards the areas of lower electron density due to the density-gradient distribution. Simultaneously, other ionized particles are relatively stationary due to the relatively large mass. Since the electrons move slower than the envelope of the laser pulse, the density of the ionized carriers is always kept identical in the forward direction. As a result, electrons are accelerated backward instead and create a dipole oriented along the laser propagation direction,^{6,7} which emits THz waves.

Specifically, at the first air/water interface, the refractive angle $\theta_r(\alpha)$ and the transmittance $T_1(\alpha)$ for a given α can be

obtained according to Snell's law and Fresnel equations, which are determined by the refractive indices of the 800-nm optical beam of air and water. The maximum $\theta_r(\alpha)$ is 48.8° when $\alpha = 90^\circ$. THz waves radiated by the dipole propagate in the water film and are attenuated due to water absorption. If the thickness of the water film is d , the absorption in different directions $\theta_t(\beta)$ from the source is described as $\exp[-\alpha_{\text{THz}}d/2\cos\theta_t(\beta)]$, where α_{THz} is the power absorption coefficient of water. Multiple reflections are neglected in the calculation due to the strong THz wave absorption in water. Additionally, the dipole radiation intensity is proportional to $\sin^2(\gamma)$, where $\gamma(\alpha, \beta) = \theta_t(\beta) - \theta_r(\alpha)$ is the angle measured with respect to the dipole direction. Then, THz waves pass through the water/air interface with a transmittance $T_2(\beta)$ and are detected by a detector. To sum up, the THz intensity angular dependence on α and β can be described as

$$I_{\text{THz}}(\alpha, \beta) \propto T_1(\alpha)T_2(\beta)\sin^2[\gamma(\alpha, \beta)] \times \exp\left(-\frac{\alpha d}{2\cos\theta_t(\beta)}\right)\left(\frac{W}{R_0}\right)^2, \quad (1)$$

where $(W/R_0)^2$ is the dipole-radiated THz power, W is the laser pulse energy, and R_0 is the radius of the plasma.⁷

Figure 2(b) plots the simulation results of the normalized THz wave intensity $I_{\text{THz}}(\alpha, \beta)$. A micro-plasma¹⁹ is created in the water film in a tightly focused geometry. It can be considered as a point source emitting THz waves. Besides

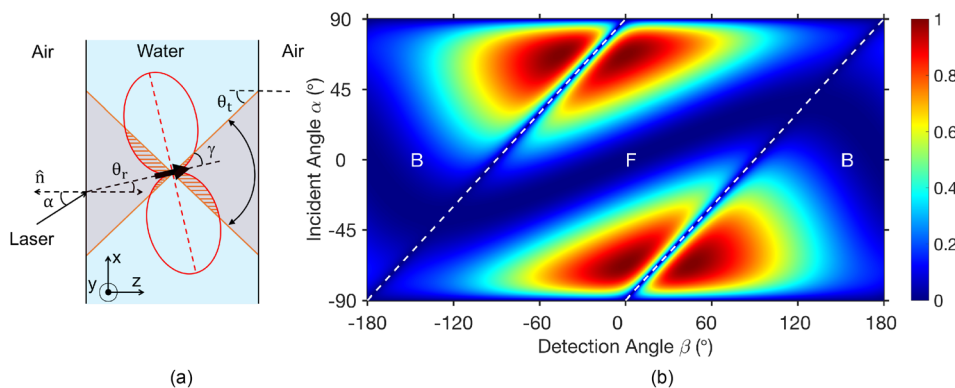


FIG. 2. (a) 2D cross-section of a dipole model approximation in a water film. Focused intense pulses are incident onto the thin water film with α and ionize water at the focal point in the direction of the refracted laser beam. The black arrow shows the dipole orientation direction. Due to the total reflection at the water/air interface, THz emission can be coupled out when $-24.6^\circ < \theta_t < +24.6^\circ$ for the waves at 0.5 THz. (b) Simulation results of normalized intensity $I_{\text{THz}}(\alpha, \beta)$ using the dipole approximation. The dashed lines indicate the cases where incidence and detection angles differ by 90° ($|\alpha - \beta| = 90^\circ$), which means that the detector is in the plane of the water film. This separates the plots into three parts, labeled as “B” and “F,” indicating the backward and forward propagating THz signals, respectively.

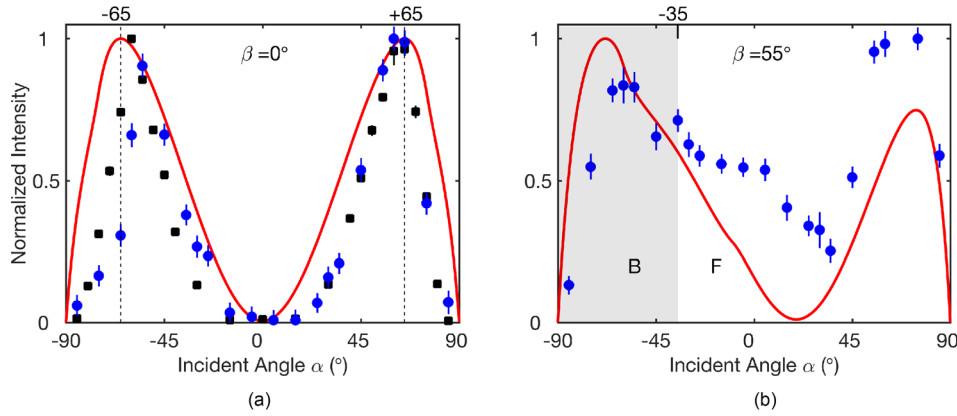


FIG. 3. THz intensity versus incidence angle α for (a) $\beta = 0^\circ$ and (b) $\beta = 55^\circ$, respectively. The black squares are the data measured by EO-sampling, and the blue dots are detected by a Golay cell. Only the forward propagating signals can be measured in (a). For $\beta = 55^\circ$, backward propagating signals are measured at $-90^\circ < \alpha < -35^\circ$.

the forward (F) propagating signal, the signal propagating in the backward (B) direction is also expected. These two parts are separated by dashed lines in the plot and labeled separately. Due to the symmetric geometry of the model, intensity distributions for forward and backward propagating THz signals have the same patterns when the plasma is in the center of the water film. The dashed lines also indicate the case of $|\alpha - \beta| = 90^\circ$, which means that the detector is placed in the plane of the water film. If $|\alpha - \beta| > 90^\circ$, the THz waves propagate in the backward direction.

To verify the simulation results, THz signal versus α is measured when β is fixed at 0° or 55° . To bring the simulation results closer to the experimental condition, integration over a solid angle (0.47π sr) is calculated for a collimating parabolic mirror with a 2-in. diameter and a 4-in. focal length. For the situation of $\beta = 0^\circ$, both EO sampling and a Golay cell are used in the measurement. The corresponding results are plotted in Fig. 3(a), where the red solid line shows the simulation results. The EO sampling results (black squares) are obtained after a temporal integration of the whole THz waveform. The results from a Golay cell are plotted as blue dots. The error is obtained by calculating the standard deviation of multiple measurements. As shown in the plot, the optimal incidence angle of the laser beam is 65° , which is a combined result of the transmittance of the p-polarized excitation laser at the air/water interface and the dipole orientation direction. Consequently, the optimal angle is thickness independent. Moreover, about 80% of energy is dissipated when $\alpha = 65^\circ$ because of the total internal reflection at the water/air interface and the strong absorption of water. In other words, THz energy should be enhanced by 5 times if the total THz energy can be coupled out when a nonpolar liquid with low absorption is used. Note that only the forward propagating THz waves can be measured when $\beta = 0^\circ$.

In general, EO sampling offers a better signal-to-noise ratio, but its optical alignment for detecting the radiation pattern is complicated. A Golay cell is a relatively direct way for the angular dependence measurement including forward and backward directions. Thus, a Golay cell is used for studying the case of $\beta = 55^\circ$ [Fig. 3(b)]. In this case, the signal comes from backward propagating THz waves instead of forward propagating parts when $-90^\circ < \alpha < -35^\circ$. Compared to the simulation results (solid line), a stronger

signal is measured in the forward propagating part. This may be a consequence of the plasma deviation from the center of the film. Nevertheless, the detectable backward propagating THz signal supports the assumption of a point source for the plasma excited by the tightly focused laser.

The linear power dependence after a threshold has been reported using a relatively low optical excitation energy range (up to 0.4 mJ).¹⁰ Here, we increase the pulse energy to 2 mJ. The THz signal increases linearly after the threshold, and no saturation is observed within this range as shown in Fig. 4. The possible reasons for the linear dependence rather than a quadratic one are understood from two aspects. On one hand, the ionized area originally at the focus will move backward by increasing the laser power because the ionization threshold is exceeded before the focus, which has been observed experimentally by previous works for the gas case.²⁰ This deviation will lead to a decrease in the THz signal due to the fact that the signal from water is critically sensitive to the relative position of the ionized plasma in the film.¹⁰ On the other hand, the THz wave intensity is also determined by the radius of the plasma (R_0) as described in Eq. (1). Because of the limitation of the film thickness and the water lower ionization potential compared with ambient air,^{13,14} the plasma in water prefers to expand in the radial direction when the edge of the ionized area reaches two interfaces, which results in an increase in R_0 . Therefore, the linear tendency could be understood by a combined result of

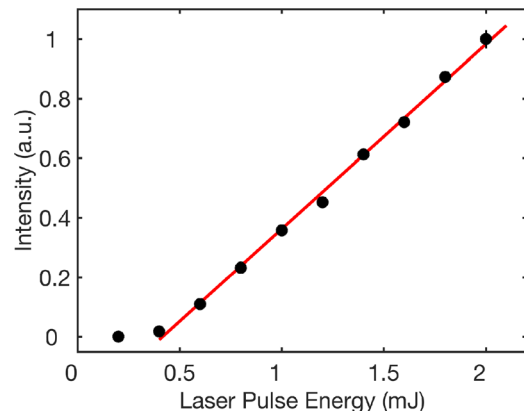


FIG. 4. Normalized THz intensity as a function of incident pulse energy when $\alpha = 65^\circ$ and $\beta = 0^\circ$. The red line shows a linear fit.

the central movement and the radial expansion of the plasma.

In summary, THz wave generation from a water film supports the ponderomotive force-induced dipole approximation. The THz waveform polarity and intensity dependence on the optical beam incidence angles at different detection angles are analyzed based on the dipole model. The optimal THz signal is confirmed when the laser incidence angle is 65° . Limited by the total internal reflection at the water/air flat interface and strong water absorption, only 20% of THz energy within the water film can be coupled out. Likely, other geometric shapes of water than the water film, such as a water line or droplet with reduced total internal reflection, could offer stronger THz signals.

The research done at the University of Rochester was sponsored by the Army Research Office under Grant No. W911NF-17-1-0428 and the Air Force Office of Scientific Research under Grant No. FA9550-18-1-0357); Tcypkin was supported by the Ministry of Education and Science of the Russian Federation (074-U01). This project was also carried out as a part of the State Assignment on Research Work for the University of Information Technology, Mechanics, and Optics at ITMO University in the Sphere of Scientific Activity.

¹S. N. Thakur and J. P. Singh, in *Laser-Induced Breakdown Spectroscopy* (Elsevier, Amsterdam, 2007).

- ²A. W. Miziolek, V. Pallechi, and I. Schechter, *Laser Induced Breakdown Spectroscopy* (Cambridge University Press, Cambridge, 2006).
- ³B. Kearton and Y. Mattley, *Nat. Photonics* **2**, 537 (2008).
- ⁴S. Corde, K. Ta Phuoc, G. Lambert, R. Fitour, V. Malka, A. Rousse, A. Beck, and E. Lefebvre, *Rev. Mod. Phys.* **85**(1), 1 (2013).
- ⁵J. Yoshii, C. H. Lai, T. Katsouleas, C. Joshi, and W. B. Mori, *Phys. Rev. Lett.* **79**(21), 4194 (1997).
- ⁶H. Hamster, A. Sullivan, S. Gordon, W. White, and R. W. Falcone, *Phys. Rev. Lett.* **71**(17), 2725 (1993).
- ⁷H. Hamster, A. Sullivan, S. Gordon, and R. W. Falcone, *Phys. Rev. E* **49**(1), 671 (1994).
- ⁸D. J. Cook and R. M. Hochstrasser, *Opt. Lett.* **25**(16), 1210 (2000).
- ⁹M. Liu, H. Y. Hwang, H. Tao, A. C. Strikwerda, K. Fan, G. R. Keiser, A. J. Sternbach, K. G. West, S. Kittiwatanakul, J. Lu et al., *Nature* **487**, 345 (2012).
- ¹⁰Q. Jin, E. Yiwen, K. Williams, J. Dai, and X.-C. Zhang, *Appl. Phys. Lett.* **111**(7), 071103 (2017).
- ¹¹I. Dey, K. Jana, V. Y. Fedorov, A. D. Koulouklidis, A. Mondal, M. Shaikh, D. Sarkar, A. D. Lad, S. Tzortzakis, A. Couairon et al., *Nat. Commun.* **8**(1), 1184 (2017).
- ¹²F. Williams, S. P. Varma, and S. Hillenius, *J. Chem. Phys.* **64**(4), 1549 (1976).
- ¹³D. N. Nikogosyan, A. A. Oraevsky, and V. I. Rupasov, *Chem. Phys.* **77**(1), 131 (1983).
- ¹⁴R. A. Crowell and D. M. Bartels, *J. Phys. Chem.* **100**(45), 17940 (1996).
- ¹⁵H. A. Hafez, X. Chai, A. Ibrahim, S. Mondal, D. Férachou, X. Ropagnol, and T. Ozaki, *J. Opt.* **18**(9), 093004 (2016).
- ¹⁶Q. Wu and X.-C. Zhang, *Appl. Phys. Lett.* **67**(24), 3523 (1995).
- ¹⁷T. Wang, P. Klarskov, and P. U. Jepsen, *IEEE Trans. Terahertz Sci. Technol.* **4**(4), 425 (2014).
- ¹⁸P. K. Kennedy, D. X. Hammer, and B. A. Rockwell, *Prog. Quantum Electron.* **21**(3), 155 (1997).
- ¹⁹F. Buccheri and X.-C. Zhang, *Optica* **2**(4), 366 (2015).
- ²⁰Y. L. Chen, J. W. L. Lewis, and C. Parigger, *J. Quant. Spectrosc. Radiat. Transfer* **67**(2), 91 (2000).